Transcriptional patterns in both host and bacterium underlie a daily rhythm of anatomical and metabolic change in a beneficial symbiosis

Andrew M. Wier[a,1], Spencer V. Nyholm[b], Mark J. Mandel[a,2], R. Prisca Massengo-Tiassé[c], Amy L. Schaefer[a,3], Irina Koroleva[d,4], Sandra Splinter-BonDurant[e], Bartley Brown[f], Liliana Manzella[d,5], Einat Snir[d], Hakeem Almabrazi[f], Todd E. Scheetz[g], Maria de Fatima Bonaldo[d,5], Thomas L. Casavant[f], M. Bento Soares[d,5], John E. Cronan[c], Jennifer L. Reed[h], Edward G. Ruby[a], and Margaret J. McFall-Ngai[a,6]

Departments of [a]Medical Microbiology and Immunology, [h]Chemical and Biological Engineering, and [e]Biotechnology Center, University of Wisconsin, Madison, WI 53706; [b]Department of Molecular and Cell Biology, University of Connecticut, Storrs, CT 06269; [c]Department of Microbiology, University of Illinois at Urbana–Champaign, Urbana, IL 61801; and Departments of [d]Pediatrics, [f]Electrical and Computer Engineering, and [g]Ophthalmology and Visual Science, University of Iowa, Iowa City, IA 52242

Edited by Everett Peter Greenberg, University of Washington, Seattle, WA, and approved December 22, 2009 (received for review August 25, 2009)

Mechanisms for controlling symbiont populations are critical for maintaining the associations that exist between a host and its microbial partners. We describe here the transcriptional, metabolic, and ultrastructural characteristics of a diel rhythm that occurs in the symbiosis between the squid *Euprymna scolopes* and the luminous bacterium *Vibrio fischeri.* The rhythm is driven by the host's expulsion from its light-emitting organ of most of the symbiont population each day at dawn. The transcriptomes of both the host epithelium that supports the symbionts and the symbiont population itself were characterized and compared at four times over this daily cycle. The greatest fluctuation in gene expression of both partners occurred as the day began. Most notable was an up-regulation in the host of >50 cytoskeleton-related genes just before dawn and their subsequent down-regulation within 6 h. Examination of the epithelium by TEM revealed a corresponding restructuring, characterized by effacement and blebbing of its apical surface. After the dawn expulsion, the epithelium reestablished its polarity, and the residual symbionts began growing, repopulating the light organ. Analysis of the symbiont transcriptome suggested that the bacteria respond to the effacement by up-regulating genes associated with anaerobic respiration of glycerol; supporting this finding, lipid analysis of the symbionts' membranes indicated a direct incorporation of host-derived fatty acids. After 12 h, the metabolic signature of the symbiont population shifted to one characteristic of chitin fermentation, which continued until the following dawn. Thus, the persistent maintenance of the squid–vibrio symbiosis is tied to a dynamic diel rhythm that involves both partners.

Euprymna scolopes | microarray | mutualism | *Vibrio fischeri* | cytoskeleton

Many symbioses begin each generation with the acquisition of their microbial partners from the surrounding environment. Once established, these "horizontally" transmitted associations are typically maintained throughout the life of the host. The persistence of the alliance requires that the partnership achieve stability, and a variety of strategies that mediate this stability have been selected over evolutionary time. With intracellular symbioses, the host must exert a strong control over symbiont proliferation. For example, in the associations between some leguminous plants and their nitrogen-fixing rhizobia, after entering and accommodating to host cells, the bacteria transform into a differentiated bacteroid state in which the symbionts are metabolically active but no longer divide (1, 2). In contrast, extracellular symbioses, such as those in animal gut tracts or light-emitting organs, often have connections to the external environment through which excess cells produced by a growing symbiont population are released (3, 4). In such symbioses, the host may assure stability by controlling symbiont number and/or activity on a daily, or "diel," rhythm (5, 6).

Recent studies have begun to find evidence of strong diel rhythms in gene expression and immune response by the cells of the mammalian gut (7, 8). These rhythms are likely to impact the intestinal microbiota and, thereby, their role in normal tissue development, efficient nutrition, and disease resistance (3); nevertheless, little is known about how the microbiota either respond to, or control, these rhythms. A better understanding of how host epithelia communicate with complex consortia to maintain a dynamic stability may reveal how they avoid dysfunctional conditions such as inflammatory bowel disease (9); however, the complex nature of enteric microbial communities make this goal challenging.

As in vertebrate enteric-tract symbioses, in the association between the Hawai'ian squid *Euprymna scolopes* and the luminous bacterium *Vibrio fischeri,* the symbiont is acquired anew each generation, and is maintained along the apical surfaces of polarized epithelia in a complex light-emitting organ (4) (Fig. 1*A*). Bioluminescence produced by the symbiont is used in the host's nocturnal behaviors, and varies in intensity over the day largely due to oxygen limitation in the organ, with the lowest levels occurring from just before dawn through early afternoon, and the highest during the night (10). Superimposed on this rhythm of light production is the diel expulsion of most of the bacterial population each dawn, followed by a period of regrowth

Author contributions: A.M.W., A.L.S., E.G.R., and M.J.M.-N. designed research; A.M.W., S.V.N., R.P.M.-T., I.K., S.S.-B., L.M., E.S., M.d.F.B., J.L.R., and E.G.R. performed research; B.B., H.A., T.E.S., T.L.C., and M.B.S. contributed new reagents/analytical tools; A.M.W., M.J.M., R.P.M.-T., I.K., S.S.-B., B.B., H.A., T.E.S., M.d.F.B., T.L.C., M.B.S., J.E.C., J.L.R., E.G.R., and M.J.M.-N. analyzed data; and A.M.W., M.J.M., E.G.R., and M.J.M.-N. wrote the paper.

The authors declare no conflict of interest.

This article is a PNAS Direct Submission.

Data deposition: The sequences reported in this paper have been deposited in the Sanger Institute Database, www.sanger.ac.uk/DataSearch, and the GenBank Expressed Sequence Tags database, www.ncbi.nlm.nih.gov/dbEST (accession nos. DW251302–DW286722).

[1]Present address: Department of Biology and Health Sciences, Pace University, Pleasantville, NY 10570.

[2]Present address: Department of Microbiology-Immunology, Northwestern University, Chicago, IL 60611.

[3]Present address: Department of Microbiology, University of Washington, Seattle, WA 98195.

[4]Present address: Novartis Institutes for Biomedical Research, Inc., Cambridge, MA 02139.

[5]Present address: Children's Memorial Research Center, Northwestern University, Chicago, IL 60614.

[6]To whom correspondence should be addressed. E-mail: mjmcfallngai@wisc.edu.

This article contains supporting information online at www.pnas.org/cgi/content/full/0909712107/DCSupplemental.

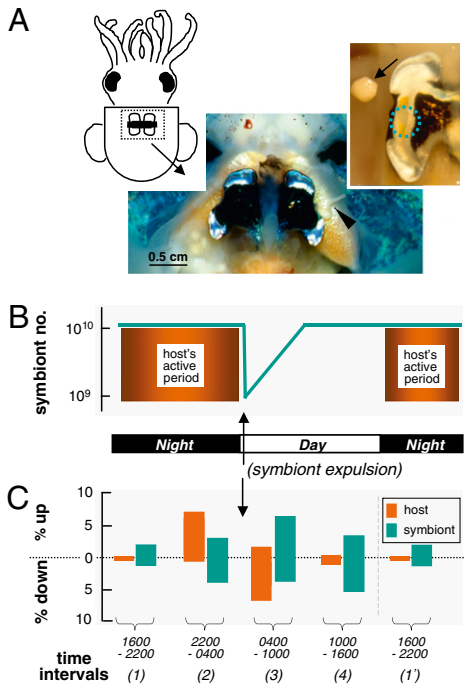

Fig. 1. The diel cycle of the squid–vibrio symbiosis. (*A*) The mature host light organ. A ventral view of the host animal (*Left*) reveals the position of the bilobed light organ in the mantle cavity. After the dawn light cue, the animal expels the crypt contents into the environment (arrowhead; ventrally dissected animal, *Center*). The central epithelial core (arrow; *Right*), which harbors the bacterial symbionts, was removed from each lobe of the organ for array analyses (approximate position indicated by dashed circle). (*B*) The night-active period of the host (orange) corresponds to the largest symbiont population (blue lines), most of which is expelled at dawn. (*C*) Differential regulation of host (orange) and symbiont (blue) genes over the day as a percentage of the total host ESTs (nonredundant cDNA library of 13,962 sequences) or symbiont genes (3,802) probed. Time intervals #1–4, regulated at: #1,1′ = 2200 hours relative to 1600 hours; #2 = 0400 hours relative to 2200 hours; #3 = 1000 hours relative to 0400 hours; #4 = 1600 hours relative to 1000 hours.

by the remaining symbionts (Fig. 1*B*). The material expelled from the light organ contains symbiotic *V. fischeri* cells embedded in a thick matrix. Analysis of this matrix has revealed a collection of amino acids and peptides mixed with an acellular, host-derived, vesicular material (11, 12). This rhythmic behavior begins at sunrise after the first day of symbiont colonization and repeats each day throughout the year-long life of the squid. How does the host epithelium orchestrate the cyclic growth and metabolic activity of its symbiont while maintaining a remarkably stable bacterial population within its tissues?

In this article, we used transcriptional analyses of both host and symbiont to characterize the molecular dialogue between the squid and its bacteria over the diel cycle. The resulting patterns of expression provided insight into cellular and physiological activities that underlie the natural, daily rhythm of this symbiosis—specifically, a daily effacement of the host epithelium and a cyclic change in anaerobic metabolism by the symbiont. These analyses demonstrate that the association has evolved a dynamic interplay between the partners that ensures the long-term stability of the association.

Results

General Gene Expression Trends Over the Diel Cycle. When levels of expression of both host and symbiont genes were compared at 6-h intervals over the daily cycle of squid activity and bacterial expulsion/regrowth, marked changes in the transcription of dozens to hundreds of genes were observed (Table S1); a total of ~10% of the ~14,000 host genes present in the EST library were regulated over four intervals of the diel cycle, and ~17% of those of the symbiont. Some periods of the day showed highly active differential regulation and others relative quiescence, although the partners differed in the magnitude and timing of this character (Fig. 1*C*). Specifically, an ~50-fold difference in the number of differentially regulated host genes occurred between the most and least active periods, whereas only an ~4-fold difference characterized the gene expression of the symbiont population. The two intervals of highest differential gene expression in host tissues occurred on either side of dawn; i.e., between 2200 and 0400 hours, which was dominated by up-regulated gene expression, and between 0400 and 1000 hours, which was dominated by down-regulated gene expression (Fig. 1*C* and Tables S1 and S2). During each of these time intervals the symbionts showed a more uniform change in the percentage of genes that were up- or down-regulated (Fig. 1*C* and Tables S1 and S3). The largest percentage of up-regulated genes in the symbionts followed that of the host; i.e., it occurred after dawn (0400–1000 hours). Analyses of the lists of differentially regulated host and symbiont genes revealed that during some intervals, both partners changed the expression of a substantial number of genes associated with metabolism and signaling (Table S4), suggesting that certain times of the day are periods of dynamic interaction between the partners.

Independent assessment of the validity of microarray results was made either by QRT-PCR confirmation of gene-expression levels and patterns, or by the presence of predicted patterns of gene co-regulation. Specifically, in the host, 10 differentially regulated genes were analyzed at all four sampling points, for a total of 40 QRT-PCR assays (Table S5). In this analysis, the level of differential regulation in the microarray was ≥2-fold in 16 of the 40 cases. In 12 of these, the microarray and QRT-PCR were differentially regulated in the same direction, often to approximately the same level of fold-change.

QRT-PCR analyses are problematic when comparing mRNA pools from different mixtures of nonisogenic bacterial strains (13), such as those present in the genetically diverse symbiont populations of light organs (14, 15). Thus, we assessed the validity of the expression patterns revealed by the symbiont array data in two other ways (*SI Methods*). We first asked whether these patterns were supported by well coordinated changes in distinct loci that are functionally linked. For example, we found that genes encoding closely linked metabolic activities (such as the formate dehydrogenase complex, or the glycerol-3-phosphate catabolism enzymes, discussed below) showed similar temporal patterns of expression (Table S6). Second, we asked whether the array data indicated that genes within an operon had the same expression behavior. As a test of this prediction, we determined that in >73% (519 of 707) of the cases, the first and second gene in a predicted operon displayed coordinate regulation. χ^2 analysis of these results rejected the null hypothesis of non-co-regulated gene expression ($P < 0.0001$). Thus, although we used pools of total mRNA from several mixed populations of *V. fischeri* symbionts to hybridize microarrays in the presence of abundant host RNA, the resulting data appeared to reliably identify at least the most robust patterns of bacterial gene expression.

Correlation of Transcriptional Patterns with Host Cellular Structure. In addition to the pre- and postdawn regulation of transcripts associated with metabolism and signaling, during the same time intervals we observed up-regulation of host immune-related genes and genes implicated in the response to stress (Table S4). Taken together, the regulation of these types of transcripts suggested significant changes in the physiology of the light-organ epithelium around dawn. Further analyses revealed an enrichment in transcripts that encode proteins of the cytoskeleton; i.e., 3.5-fold greater than expected. Specifically, when the 32 cytos-

keletal gene families present in the squid EST database (16) were analyzed, 23 (72%) of these were found to include genes that were differentially regulated across the diel cycle (Fig. 2*A*); 93% of the genes in these 23 families displayed the same dramatic pattern of regulation over the two time intervals (#2 and #3) just before and after dawn (Fig. 2*A* and Fig. S1).

This indication of cytoskeletal activity led us to examine the epithelium of the light-organ crypts by TEM at different times over the day–night cycle. For most of each 24-h period, the crypt epithelium is characteristic of that of healthy tissue: highly polarized, with lobate microvilli interfacing closely with the bacterial population (Fig. 2*B*). However, in the hours right around dawn, these epithelial cells become effaced, and their apical surfaces appear to bleb into the crypts (Fig. 2*C*) in a manner similar to tissues colonized by enteropathogens (17). The presence of host-cell membrane vesicles was most apparent after the dawn expulsion of bacteria (Fig. 1*B*), when the symbiont population is at its lowest level and is preparing to proliferate back to its normal size. Remarkably, within a few hours, an ordered microvillar border has been restored to the epithelium, and the light-organ crypts are again fully colonized by bacterial symbionts.

Correlation of Transcriptional Patterns with Symbiont Metabolism. To better understand the metabolic activity that underlies reproliferation of the symbiont population each morning, we examined the changes in bacterial gene expression that occurred over the day–night cycle (Table S3). A number of distinct metabolic patterns appeared, especially during the intervals around dawn. Just before expulsion (interval #2; 2200–0400 hours),

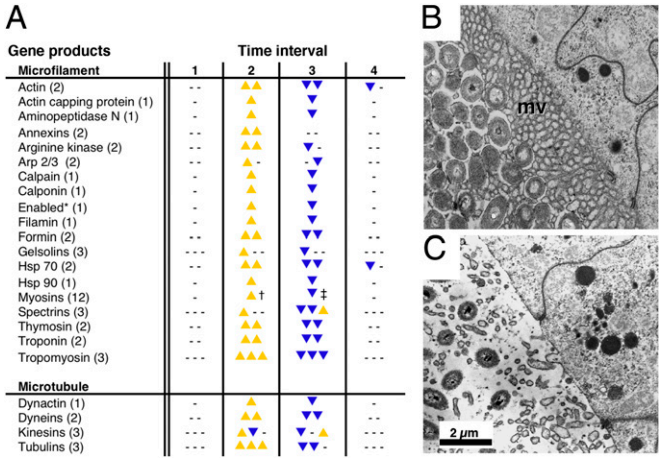

Fig. 2. The diel pattern of host cytoskeletal dynamics. (*A*) Differential regulation (based on per-spot per-chip (PSPC) values of $P < 0.05$) of cytoskeletal (i.e., microfilament- and microtubule-associated) genes over the time intervals examined: #1 = 2200 hours relative to 1600 hours; #2 = 0400 hours relative to 2200 hours; #3 = 1000 hours relative to 0400 hours; #4 = 1600 hours relative to 1000 hours. The number of regulated microarray features (genes) with a given annotation are in parentheses. *, genes regulated when the stringency was relaxed to PSPC values of $P < 0.1$; †, 11 genes were not significantly regulated, and one was significantly up-regulated; ‡, 11 genes were significantly down-regulated, and one was not significantly regulated. (*B* and *C*) TEMs of the apical surfaces of host crypt epithelia (upper right of each image) and the bacteria-containing crypt space (lower left of each image). (*B*) From the late morning through the evening time periods, a dense bacterial population associates closely with the lobate microvilli (mv) of the highly polarized host epithelia. (*C*) In the hours surrounding dawn, the host cell membranes are effaced of microvilli, and portions of the apical surfaces of these cells bleb into the bacteria-containing crypt spaces. This specific micrograph depicts host tissues right after the expulsion process, when population densities of the symbiont have not yet recovered.

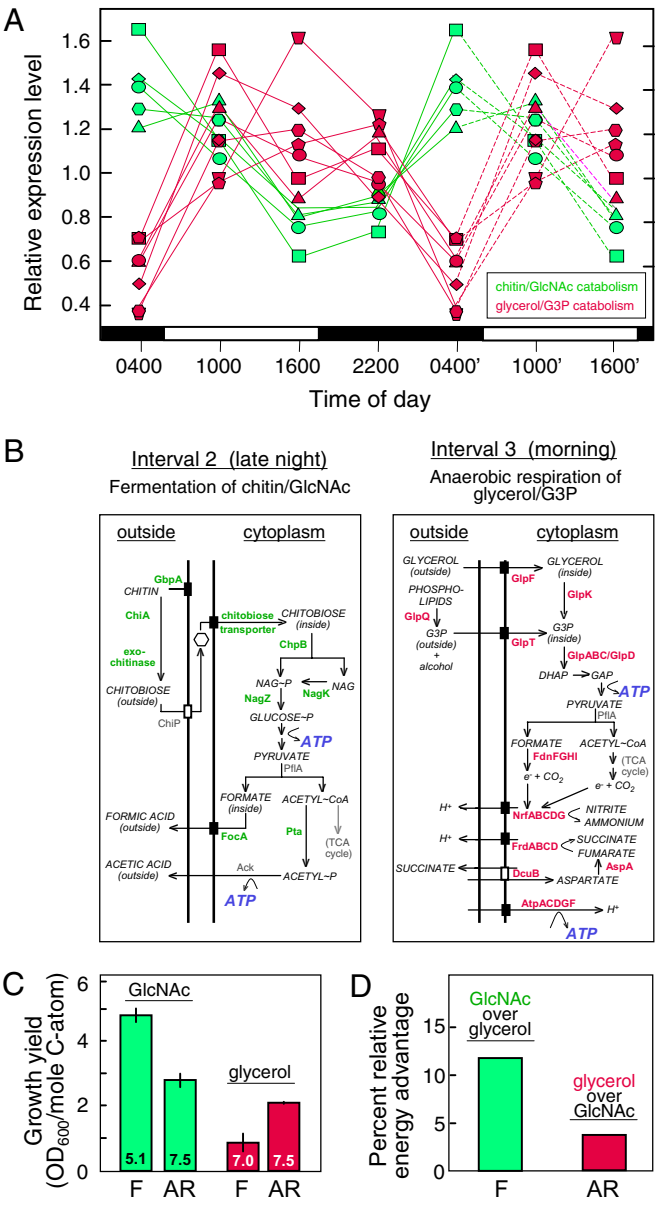

Fig. 3. Evidence of a diel pattern of symbiont metabolism. (*A*) Sequential expression of two groups of catabolic genes. Genes involved in either chitin utilization (light green) or glycerol utilization (magenta) are coordinately transcribed at peak levels during either the late night (interval #2; 2200–0400 hours) or morning (interval #3; 0400–1000 hours), respectively. Chitin genes include: circles, *VF_0655*; squares, *VF_1598*; triangles, *VF_A0013*; diamonds, *VF_A0143*; and hexagons, *VF_A0715*. Glycerol genes include: circles, *VF_0072*; squares, *VF_A0235*; triangles, *VF_A0236*; diamonds, *VF_A0248*; hexagons, *VF_A0249*; trapezoids, *VF_A0250*; and pentagons, *VF_A0958*. The relatively small, although statistically significant, fold-changes seen here have been noted in other studies of natural populations of genetically dissimilar strains (25). (*B*) Coordinate expression of distinct catabolic pathways. Proteins required for generation of ATP by the fermentation of chitin (left panel) or anaerobic respiration of glycerol or G3P (right panel) are indicated. Proteins that are apparently induced during Interval #2 or #3 [e.g., those in (A)] are indicated in light green or magenta, respectively. DHAP, dihydroxyacetone phosphate; GAP, glyceraldehyde phosphate; GlcNAc, *N*-acetyl glucosamine. (*C*) Metabolic capabilities of *V. fischeri* in culture. Growth yields per mole of substrate carbon [GlcNAc (light green bars) or glycerol (magenta bars)] in minimal-salts medium (52), and final pHs (indicated on the bars) were determined when cells were grown either fermentatively (F) with no electron acceptor or by anaerobic nitrate respiration (AR). (*D*) The relative energy-generation advantage of growth on GlcNAc relative to glycerol (light green bar) or glycerol relative to GlcNAc (magenta bar) were calculated by using a metabolic model based on the substrate-specific efficiency of ATP generation by fermentation or anaerobic respiration (18).

there was a clear increase in expression of the genes required for the catabolism of chitin and its monomeric derivative, GlcNAc (Fig. 3*A*). For example, genes encoding secreted chitinases, subunits of the chitobiose-specific transporter, and enzymes required to funnel GlcNAc into glycolysis were up-regulated (Table S6), suggesting that energy generation before dawn is driven by chitin fermentation, which is predicted to result in acidic by-products (Fig. 3*B*). In contrast, just after expulsion (interval #3; 0400–1000 hours), chitin-utilization genes were down-regulated and remained depressed until the onset of night, whereas the genes associated with glycerol and G3P catabolism were up-regulated (Fig. 3*A* and Table S6). Similarly, after dawn the symbionts induced genes associated with the anaerobic respiration (rather than fermentation) of glycerol, including formate dehydrogenase (Fdn), formate-dependent NO/nitrite reductase (Nrf), and a fumarate reductase (Frd), which is supported by an anaerobic succinate-aspartate antiporter system (DcuB/AspA) that supplies substrate to this reductase and removes its product (Fig. 3*B*). Harvesting the resultant protonmotive force, the bacterium appears to use its ATPase to generate energy anaerobically from glycerol in a pH-neutral manner. The ability of the bacteria to perform these predicted metabolic activities was confirmed in culture (Fig. 3*C*). Interestingly, when using GlcNAc, *V. fischeri* has a higher cell yield growing fermentatively; in contrast, when glycerol is the carbon source, the bacterium grows more effectively by anaerobic respiration.

One possible reason that the symbionts might shift their metabolism (i.e., from GlcNAc fermentation, to glycerol anaerobic respiration, and back again) would be that the two substrates are more efficiently converted to ATP by using these two different forms of anaerobic metabolism. To test this hypothesis, we modified an existing metabolic flux model for *Escherichia coli* (18) to better reflect *V. fischeri* metabolism (19), and used it to estimate ATP production from different substrates. When the energy efficiency (i.e., ATP formed per carbon atom in the substrate) was mathematically analyzed using this model, it was predicted that under fermentation conditions GlcNAc would yield 12% more energy per carbon atom than glycerol (Fig. 3*D*). Conversely, under conditions of anaerobic respiration, glycerol would out-yield GlcNAc. Thus, only if electron acceptors are unavailable will utilization of GlcNAc for ATP production be energetically more favorable than using glycerol. Although the nutritional conditions within the light organ remain unknown, taken together these calculations support the possibility that over the course of a 24-h period, the host provides different substrates to its symbionts to optimize their performance under the changing physiological conditions present in its tissues over the day–night cycle.

The temporal patterns of host and symbiont gene expression, as well as the coinciding change in the morphology of the epithelium, led us to hypothesize that after the host expels most of the symbiont population at dawn, the remaining bacteria repopulate the light organ by metabolizing the host-derived lipid vesicles surrounding them (Fig. 2*C*). Such vesicular membrane material would be a rich source of glycerophospholipids, from which glycerol and G3P could be released by the activity of an induced periplasmic GlpQ (Fig. 3*B*). We reasoned that the fatty acids freed from these host vesicles would be available for incorporation directly into bacterial membrane lipids, leaving a record of their source. Consistent with this prediction, we found that the symbiont's lipid profile was distinct from that of culture-grown *V. fischeri*; that is, it included not only the de novo-synthesized fatty acids (e.g., 16:1) characteristic of these bacteria, but also a subset of long-chain fatty acids (e.g., 20:4 and 22:6) characteristic of those found in host lipids (Fig. 4).

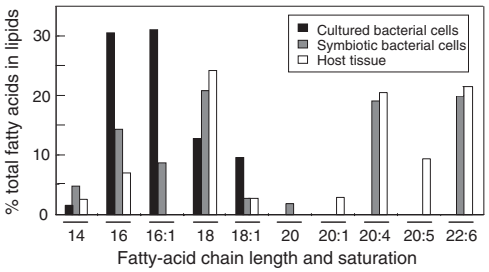

Fig. 4. Fatty-acid composition of bacterial symbionts. The chain length, saturation, and relative amount of each of the fatty acids present in the lipids of symbiotic bacteria purified directly from the light organ (gray bars) were compared with those of the same bacteria subsequently grown in medium (black bars) or with those of the light-organ epithelial tissue (open bars).

Discussion

Dual-transcriptome studies of microbes and their hosts have been used to analyze both pathogenic (20) and, more rarely, beneficial associations (21–23). We report here determinations of synchronous gene-expression patterns for both partners of a symbiosis over the course of a day–night cycle. Another major difference between this study and those of others is the use of naturally occurring animal hosts. Although not as technically robust as analyses of laboratory-grown subjects, studies using wild-caught organisms better capture a view of how the association functions in nature. However, only pronounced changes in gene expression may be detected because mRNA isolated from natural populations of hosts and symbionts represents a mixture of alleles (15, 24). Such mixtures will imperfectly match the array's oligonucleotide probes and may lead to the atypically low (<2-fold), but consistent, level of fold-change in gene expression found here (e.g., Fig. 3*A*) and with other natural samples, such as *V. cholerae* in human stools (25). Nevertheless, we show that, even with such genetic averaging, transcriptional examination of a natural symbiotic population can reveal statistically significant signals and drive the discovery of prominent biological processes and relationships.

One such discovery is that homeostasis in the squid–vibrio symbiosis is not achieved simply by maintaining a steady state set point, but rather involves a daily transformation of the microanatomy of host tissues and a corresponding set of transcriptional changes in both partners. The data demonstrate that, similar to many biological functions in animals, the symbiosis is controlled on a complex daily rhythm. This rhythm provides a mechanism for controlling the symbiont population's size and activity, apparently contributing to the maintenance of a stable, long-term association.

Based on the results presented here, we have begun to build a model of the complex interactions that support this association. Transcriptional analyses provide evidence that each day the symbiont cycles through at least two distinct metabolic states in response to different nutrient sources provided by the host (Fig. 3*A*). Both of these predicted states are consistent with the oxygen-limited conditions present in the light organ (10). After dawn, and throughout the daylight hours, the bacteria appear to respire nitrate/nitrite anaerobically (Fig. 3*B*), using G3P derived from host membrane vesicles as a substrate. Supporting this hypothesis, 21 of 24 *Vibrio* genes that have been predicted from bioinformatics to be regulated by the nitrite-responsive elements NarPQ during anaerobic respiration (26) have an increased expression in the symbionts during the morning. A number of pathogens, including *V. cholerae*, also apparently respire nitrate/nitrite when host-associated, and this metabolism plays a critical, but as yet uncharacterized, role in their virulence (27–29). The source of

nitrate/nitrite in these associations is not known; however, in the squid host it may come from a spontaneous oxidation of NO produced by the light-organ epithelium (30).

At night, a down-regulation of anaerobic-respiration genes occurs concomitantly with an up-regulation of the expression of genes associated with the fermentative catabolism of chitin (Fig. 3*B*), a structural molecule in squid tissue that has been associated with initiation of the symbiosis (31). Thus, chitin appears to replace G3P as a nutrient during the period when the symbiont population is not increasing and luminescence is maximal (10). The number of genes with changes in level of expression during this replacement is consistent with that reported for *E. coli* changing from acetate to glucose metabolism (32).

The hypothesis that, in the squid–vibrio symbiosis, one of the purposes for the cyclic changes in host tissue structure is to periodically provide the symbionts with membrane-derived glycerol and fatty acids (Fig. 4) is not without precedent. In certain pathogenic associations, epithelial cytoskeletal events such as effacement are bacteria-induced (33), and host membrane-derived fatty acids may be directly incorporated by the pathogen (34). Thus, these parallels in the ways beneficial and pathogenic bacteria interact with their hosts join a growing list of functional similarities in the mechanisms underlying animal–bacteria associations (21–23, 35–38).

A daily program of profound modification of the anatomy and behavior of the host epithelium may not be unique to the squid–vibrio symbiosis. Most notably, multiple lines of transcriptional and anatomical evidence emerging from mammalian systems (39) suggest that symbioses between gut consortia and their supporting host tissues may be similarly controlled. Transcriptional profiling of the murine distal colon has shown that gene expression in these tissues is circadian: >1,200 genes (3.7% of the mouse genome) exhibit rhythmic expression profiles (8). There are also strong biological rhythms in gene expression of the immune system of the small intestine (7). In addition, a recent study of the brush border of healthy mammalian enterocytes has reported that these cells periodically bleb their apical surfaces, releasing vesicles into the gastrointestinal lumen (40), although it was not determined whether this release occurs on a diel rhythm. As of yet, it is not known whether the normal microbiota either induce or benefit from any of these processes. However, because the normal microbiota work in concert with the epithelial and immune cells in the regulation of homeostasis (41, 42), it seems likely that the activities of symbiont populations in the enteric tract will mirror these phenomena and, perhaps, play a significant role in the association's dynamic stability. Our results suggest parallels between events occurring in the mammalian intestine and in the squid light organ (43). If these parallels exist, the maintenance of host–microbe stability would join the array of other complex animal behaviors that are controlled by diel rhythms.

Methods

Tissue Preparation for Microarray Analyses. Adult *E. scolopes* squid were collected on leeward Oahu, Hawai'i, transferred to outdoor tanks to maintain natural light cues, and allowed to recover for at least 1 week before sacrifice. Animals were anesthetized in 2% ethanol in seawater at four times over the day–night cycle (0400, 1000, 1600, and 2200 hours) and ventrally dissected, and the central cores of their light organs (Fig. 1*A*) were removed into RNAlater (Ambion) for microarray analyses (*SI Methods*).

Microarray Hybridizations and Analyses. Total RNA, containing both host and symbiont contributions, was isolated from sets of light-organ central cores (*SI Methods*). For the study of host gene expression, spotted glass microarrays were prepared from a nonredundant cDNA library containing 13,962 sequences, obtained from juvenile squid light organs (16). Symbiont gene expression was determined by using a whole-genome custom GeneChip microarray (Affymetrix) designed from the *V. fischeri* ES114 genome (44). For each of the four time-point samples, the hybridization signals were normalized by Affymetrix software (total signal per array = 10,000,000) to correct for different amounts of symbiont RNA in each sample (*SI Methods*). We sorted for genes that showed >1.5-fold differential regulation between at least two consecutive time points, with $P < 0.01$. The relatively low fold-change values are consistent with the levels found in other transcriptional analyses of naturally occurring mixed-strain populations (25, 45, 46).

Validation of Array Analyses. To verify the differential expression of genes identified in the host array analyses, QRT-PCR was performed on selected transcripts (Table S5) from the same RNA pools used in the arrays (*SI Methods*). We analyzed the reliability of the symbiont array data as follows: operon predictions for the *V. fischeri* ES114 genome (47) were independently obtained from the DOOR database (48). Within a normalized dataset, we limited our analysis to operons in which the first (5′-most) gene displayed a >1.5-fold change in expression across at least one of the time intervals in the study. Among these candidate operons, we determined whether the second gene in the operon demonstrated the same direction of change as the first.

Transmission Electron Microscopy of Host Tissue. For TEM, whole light organs were prepared by using a modification of the method described in ref. 49 (*SI Methods*). Samples were fixed and embedded at different times over the day–night cycle and examined for ultrastructural cytoskeletal changes.

Preparation of Symbionts and Host Tissue for Fatty Acid Analysis. The fatty-acid compositions of purified symbiont-free host tissue, the tissue-free symbiont cells (removed from adult animals at noon), and cultured bacteria (*SI Methods*) were determined by gas chromatography/mass spectrometry (GC/MS) as described in ref. 50. Control bacterial purifications were performed on mixtures of culture-grown *V. fischeri* cells and symbiont-free host tissues. Lipid extraction and analysis of these preparations revealed only bacterial fatty acids; essentially no host-tissue contamination was detected.

Metabolic Modeling of Symbionts. A constraint-based metabolic model developed for *Escherichia coli* K-12 (18) was modified to identify genes in *V. fischeri* required for growth on either glycerol or GlcNAc under anaerobic conditions. We eliminated 350 genes (and their corresponding reactions) from the *E. coli* model when no orthologous gene could be found in *V. fischeri*. Nitrate reductase reactions were also added based on the genome annotation for *V. fischeri* (19). A flux-balance analysis (51) was then used to calculate the predicted maximum ATP production for each substrate, assuming an input of 10 mmol of carbon source/g dry weight/h.

ACKNOWLEDGMENTS. We thank E. Heath-Heckman and N. Bekiares for comments on the manuscript. This work was supported by grants from the W. M. Keck Foundation (to M.M.-N. and E.G.R.), National Institutes of Health Grants R01-RR12294 (to E.G.R.) and R01-AI50661 (to M.M.-N.), and National Science Foundation Grants IOS 0817232 (to M.M.-N. and E.G.R.) and IOS 0715905 (to M.M.-N.). M.J.M. was supported by a National Research Service Award from the National Institute of General Medical Sciences, and R.P.M.-T. was supported by National Institutes of Health Grant R01-AI15650 (to J.E.C.). This is Contribution 1362 of the Hawai'i Institute of Marine Biology, University of Hawaii.

1. Gibson KE, Kobayashi H, Walker GC (2008) Molecular determinants of a symbiotic chronic infection. *Annu Rev Genet* 42:413–441.
2. Oke V, Long SR (1999) Bacteroid formation in the *Rhizobium*-legume symbiosis. *Curr Opin Microbiol* 2:641–646.
3. Bäckhed F, Ley RE, Sonnenburg JL, Peterson DA, Gordon JI (2005) Host-bacterial mutualism in the human intestine. *Science* 307:1915–1920.
4. Nyholm SV, McFall-Ngai MJ (2004) The winnowing: establishing the squid-*vibrio* symbiosis. *Nat Rev Microbiol* 2:632–642.
5. Flint JF, Drzymalski D, Montgomery WL, Southam G, Angert ER (2005) Nocturnal production of endospores in natural populations of *epulopiscium*-like surgeonfish symbionts. *J Bacteriol* 187:7460–7470.
6. Rees AV, Fitt WK, Baillie B, Yellowlees D (1993) A method for temporal measurement of hemolymph composition in the giant clam symbiosis and its application to glucose and glycerol levels during a diel cycle. *Limnol Oceanogr* 38:203–217.
7. Froy O, Chapnik N (2007) Circadian oscillation of innate immunity components in mouse small intestine. *Mol Immunol* 44:1954–1960.
8. Hoogerwerf WA, et al. (2008) Transcriptional profiling of mRNA expression in the mouse distal colon. *Gastroenterology* 135:2019–2029.
9. Andoh A, Benno Y, Kanauchi O, Fujiyama Y (2009) Recent advances in molecular approaches to gut microbiota in inflammatory bowel disease. *Curr Pharm Des* 15: 2066–2073.

10. Boettcher KJ, Ruby EG, McFall-Ngai MJ (1996) Bioluminescence in the symbiotic squid *Euprymna scolopes* is controlled by a daily biological rhythm. *J Comp Physiol A* 179:65–73.
11. Graf J, Ruby EG (1998) Host-derived amino acids support the proliferation of symbiotic bacteria. *Proc Natl Acad Sci USA* 95:1818–1822.
12. Nyholm SV, McFall-Ngai MJ (1998) Sampling the light-organ microenvironment of *Euprymna scolopes*: description of a population of host cells in association with the bacterial symbiont *Vibrio fischeri*.. *Biol Bull* 195:89–97.
13. Smith CJ, Osborn AM (2009) Advantages and limitations of quantitative PCR (Q-PCR)-based approaches in microbial ecology. *FEMS Microbiol Ecol* 67:6–20.
14. Mandel MJ, Wollenberg MS, Stabb EV, Visick KL, Ruby EG (2009) A single regulatory gene is sufficient to alter bacterial host range. *Nature* 458:215–218.
15. Wollenberg MS, Ruby EG (2009) Population structure of *Vibrio fischeri* within the light organs of *Euprymna scolopes* squid from Two Oahu (Hawaii) populations. *Appl Environ Microbiol* 75:193–202.
16. Chun CK, et al. (2006) An annotated cDNA library of juvenile *Euprymna scolopes* with and without colonization by the symbiont *Vibrio fischeri*. *BMC Genomics* 7:154.
17. Potter DA, et al. (2003) Calpain regulates enterocyte brush border actin assembly and pathogenic *Escherichia coli*-mediated effacement. *J Biol Chem* 278:30403–30412.
18. Reed JL, Vo TD, Schilling CH, Palsson BO (2003) An expanded genome-scale model of *Escherichia coli* K-12 (iJR904 GSM/GPR). *Genome Biol* 4:R54.
19. Ruby EG, et al. (2005) Complete genome sequence of *Vibrio fischeri*: a symbiotic bacterium with pathogenic congeners. *Proc Natl Acad Sci USA* 102:3004–3009.
20. Guerfali FZ, et al. (2008) Simultaneous gene expression profiling in human macrophages infected with *Leishmania major* parasites using SAGE. *BMC Genomics* 9:238.
21. Barnett MJ, Toman CJ, Fisher RF, Long SR (2004) A dual-genome Symbiosis Chip for coordinate study of signal exchange and development in a prokaryote-host interaction. *Proc Natl Acad Sci USA* 101:16636–16641.
22. Mahowald MA, et al. (2009) Characterizing a model human gut microbiota composed of members of its two dominant bacterial phyla. *Proc Natl Acad Sci USA* 106: 5859–5864.
23. Wilson AC, et al. (2006) A dual-genome microarray for the pea aphid, *Acyrthosiphon pisum*, and its obligate bacterial symbiont, *Buchnera aphidicola*. *BMC Genomics* 7:50.
24. Kimbell JR, McFall-Ngai MJ, Roderick G (2002) Two genetically distinct populations of bobtail squid, *Euprymna scolopes,* exist on the island O'ahu. *Pac Sci* 56:347–355.
25. Larocque RC, et al. (2005) Transcriptional profiling of *Vibrio cholerae* recovered directly from patient specimens during early and late stages of human infection. *Infect Immun* 73:4488–4493.
26. Ravcheev DA, Gerasimova AV, Mironov AA, Gelfand MS (2007) Comparative genomic analysis of regulation of anaerobic respiration in ten genomes from three families of gamma-proteobacteria (Enterobacteriaceae, Pasteurellaceae, Vibrionaceae). *BMC Genomics* 8:54.
27. Palmer KL, Brown SA, Whiteley M (2007) Membrane-bound nitrate reductase is required for anaerobic growth in cystic fibrosis sputum. *J Bacteriol* 189:4449–4455.
28. Weber I, Fritz C, Ruttkowski S, Kreft A, Bange FC (2000) Anaerobic nitrate reductase (*narGHJI*) activity of *Mycobacterium bovis* BCG i*n vitro* and its contribution to virulence in immunodeficient mice. *Mol Microbiol* 35:1017–1025.
29. Xu Q, Dziejman M, Mekalanos JJ (2003) Determination of the transcriptome of *Vibrio cholerae* during intraintestinal growth and midexponential phase *in vitro*. *Proc Natl Acad Sci USA* 100:1286–1291.
30. Davidson SK, Koropatnick TA, Kossmehl R, Sycuro L, McFall-Ngai MJ (2004) NO means 'yes' in the squid-vibrio symbiosis: nitric oxide (NO) during the initial stages of a beneficial association. *Cell Microbiol* 6:1139–1151.
31. Mandel MJ, Schaefer AL, Brennan C, Graber JR, DeLoney-Marino C, Ruby EG (in review) Ringing the dinner bell: chitin oligosaccharides as nutrients and chemotactic signals in the squid-vibrio symbiosis. *Cell Host Microbe*.
32. Kao KC, Tran LM, Liao JC (2005) A global regulatory role of gluconeogenic genes in *Escherichia coli* revealed by transcriptome network analysis. *J Biol Chem* 280: 36079–36087.
33. Gruenheid S, Finlay BB (2003) Microbial pathogenesis and cytoskeletal function. *Nature* 422:775–781.
34. McElhaney RN (1992) *Mycoplasmas: molecular biology and pathogenesis*, eds McElhaney RN, Finch LR, Baseman JB (ASM Press, Washington, DC), pp 231–258.
35. Hooper LV, et al. (2001) Molecular analysis of commensal host-microbial relationships in the intestine. *Science* 291:881–884.
36. Koropatnick TA, et al. (2004) Microbial factor-mediated development in a host-bacterial mutualism. *Science* 306:1186–1188.
37. Parsek MR, Greenberg EP (2000) Acyl-homoserine lactone quorum sensing in gram-negative bacteria: a signaling mechanism involved in associations with higher organisms. *Proc Natl Acad Sci USA* 97:8789–8793.
38. Rawls JF, Samuel BS, Gordon JI (2004) Gnotobiotic zebrafish reveal evolutionarily conserved responses to the gut microbiota. *Proc Natl Acad Sci USA* 101:4596–4601.
39. Hoogerwerf WA, et al. (2007) Clock gene expression in the murine gastrointestinal tract: endogenous rhythmicity and effects of a feeding regimen. *Gastroenterology* 133:1250–1260.
40. McConnell RE, et al. (2009) The enterocyte microvillus is a vesicle-generating organelle. *J Cell Biol* 185:1285–1298.
41. Gordon JI, Hooper LV, McNevin MS, Wong M, Bry L (1997) Epithelial cell growth and differentiation. III. Promoting diversity in the intestine: conversations between the microflora, epithelium, and diffuse GALT. *Am J Physiol* 273:G565–G570.
42. Round JL, Mazmanian SK (2009) The gut microbiota shapes intestinal immune responses during health and disease. *Nat Rev Immunol* 9:313–323.
43. Chun CK, et al. (2008) Effects of colonization, luminescence, and autoinducer on host transcription during development of the squid-vibrio association. *Proc Natl Acad Sci USA* 105:11323–11328.
44. Antunes LC, et al. (2007) Transcriptome analysis of the *Vibrio fischeri* LuxR-LuxI regulon. *J Bacteriol* 189:8387–8391.
45. Mahadav A, Gerling D, Gottlieb Y, Czosnek H, Ghanim M (2008) Parasitization by the wasp *Eretmocerus mundus* induces transcription of genes related to immune response and symbiotic bacteria proliferation in the whitefly *Bemisia tabaci*. *BMC Genomics* 9:342.
46. Son MS, Matthews WJ, Jr, Kang Y, Nguyen DT, Hoang TT (2007) In vivo evidence of *Pseudomonas aeruginosa* nutrient acquisition and pathogenesis in the lungs of cystic fibrosis patients. *Infect Immun* 75:5313–5324.
47. Mandel MJ, Stabb EV, Ruby EG (2008) Comparative genomics-based investigation of resequencing targets in *Vibrio fischeri*: focus on point miscalls and artefactual expansions. *BMC Genomics* 9:138.
48. Mao F, Dam P, Chou J, Olman V, Xu Y (2009) DOOR: a database for prokaryotic operons. *Nucleic Acids Res* 37 (Database issue):D459–D463.
49. McFall-Ngai MJ, Montgomery MK (1990) The anatomy and morphology of the adult bacterial light organ of *Euprymna scolopes* Berry (Cephalopoda: Sepiolidae). *Biol Bull* 179:332–339.
50. Fang J, Kato C, Sato T, Chan O, McKay D (2004) Biosynthesis and dietary uptake of polyunsaturated fatty acids by piezophilic bacteria. *Comp Biochem Physiol B Biochem Mol Biol* 137:455–461.
51. Price ND, Reed JL, Palsson BO (2004) Genome-scale models of microbial cells: evaluating the consequences of constraints. *Nat Rev Microbiol* 2:886–897.
52. Ruby EG, Nealson KH (1977) Pyruvate production and excretion by the luminous marine bacteria. *Appl Environ Microbiol* 34:164–169.